View metadata, citation and similar papers at core.ac.uk
brought to you by CORE
provided by Ghent University Academic Bibliography

Specular and Diffuse Reflectance of Phase-Separated Polymer Blend Films

Asritha Nallapaneni, Matthew D. Shawkey,* Alamgir Karim*

Diffuse reflectors have various applications in devices ranging from liquid crystal displays to light emitting diodes, to coatings. Herein, specular and diffuse reflectance from controlled phase separation of polymer blend films, a well-known self-organization process, are studied. Temperature-induced spinodal phase separation of polymer blend films in which one of the components is selectively extracted is shown to exhibit enhanced surface roughness as compared to unextracted films, leading to a notable increase of diffuse reflectance. Diffuse reflectance of UV–visible light from such selectively leached phase-separated blend films is determined by a synergy of varying lateral scale of phase separation (≈200 nm to 1 μm) and blend film surface roughness (0–40 nm). These critical parameters are controlled by tuning annealing time (0.5–3 h) and temperature (140, 150, 160 °C) of phase separation. Angle-resolved diffuse reflection studies show that the surface-roughened polymer films exhibit diffuse reflectance up to 40° from normal incident light in contrast to optically uniform as-cast films that exhibit largely specular reflectance. Furthermore, the intensity of the diffusively reflected light can be enhanced (300–700 nm) or reduced (220–300 nm) significantly by coating the leached phase-separated films with a thin silver over layer.

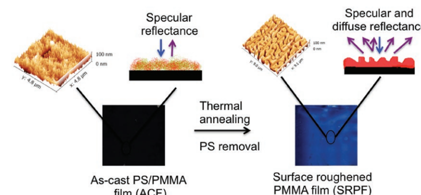

1. Introduction

Diffuse reflectors are used in numerous applications such as the back-lit units of liquid crystal display panels[1] (LCD) to enable uniform distribution of light, light emitting diodes[2–5] (LED) to enhance light extraction efficiency, solar cell devices[6,7] to increase light trapping, and in coatings[8] to reduce gloss. Surfaces with controlled roughness at the air/film interface can control diffuse reflection by omnidirectional scattering of light.[9–12] This concept has been realized via fabrication of diffuse reflectors through vacuum deposition of metals,[13] as well as via 3D lithography techniques.[14] Similarly, surface-roughened nanostructures can enhance the efficiency of light extraction in LED devices.[15–18] Other methods involve the use of nanoparticle assembly on polyelectrolyte multilayers to enhance diffuse reflectance.[19] However, all of these methods are relatively expensive for large-scale production of diffuse reflectors. Hence, a self-assembly technique that offers control over surface feature dimensions would be a desirable alternative to control diffuse reflectance. This is not unlike use of self-assembly processes such as block copolymer phase separation[20–22] and polymerization-induced phase separation[23] for optical applications. Indeed, polymer-blend-based nanopillar morphologies were recently studied for their applicability to LEDs.[24,25] In this regard, phase separation in polymer blend films

A. Nallapaneni, Prof. A. Karim
Department of Polymer Engineering
University of Akron
250 S Forge Street, OH 44325, USA
E-mail: alamgir@uakron.edu
Prof. M. D. Shawkey
Department of Biology
University of Ghent
Ledganckstraat 35, Ghent 9000, Belgium
E-mail: Matthew.Shawkey@UGent.be

Macromol. Rapid Commun. **2017**, *38*, 1600803
© 2017 WILEY-VCH Verlag GmbH & Co. KGaA, Weinheim

DOI: 10.1002/marc.201600803

may be a useful self-assembly approach, as the length scales of phase separation in polymer blends can span the full range of optical wavelengths, making them suitable for artificially inducing diffuse reflectance from polymer films. Notably, a key advantage is that a polymer blend thin-film-based diffuse reflector fabrication technique is advantageous because it is compatible with a roll-to-roll (R2R) process, facilitating large-scale processing for future flexible electronic applications.

Spinodal dewetting and decomposition in polymers has been used to obtain patterned substrates and generation of hierarchial meso, macroporous carbon.[26,27] However, little is known about the optical activity of phase-separated structures through spinodal decomposition that produce nanoroughened polymer blend films over a wide range of scale of phase separation.[28,29] The aim of this study is to understand and correlate the specular and diffuse reflectance of spinodally phase-separated polymer blend thin films with thermal processing parameters. Phase separation in polymer blend films depends on the interaction parameter between the polymer blend components and annealing conditions, including thermal quench depth relative to phase boundary and annealing time,[30] finite size effects of film thickness,[31] preferential substrate interactions of polymer blend components,[32] quality and volatility of casting solvent, and interactions with substrate and blend components.[33] Temperature-induced phase separation of polymer blend films, after which one of the constituents is selectively removed after phase separation, offers a promising route to impart surface roughness. For example, phase separation in a lower critical solution temperature deuterated-polystyrene/polyvinylmethylether system and upper critical solution temperature (UCST) polystyrene/polymethylmethacrylate (PS/PMMA) polymer blend thin films results in surface roughness that, in turn, depends on annealing conditions.[30,34] We used PS/PMMA as a model system in this study because phase separation in PS/PMMA blend films is extensively studied,[30,31,35,36] and it exhibits UCST.

2. Experimental Section

2.1. Materials, Film Casting, and Imaging

3 wt% PS (M_n: 10.5 kg mol^{-1}; polydispersity index (PDI): 1.3) and PMMA (M_n: 3.1 kg mol^{-1}; PDI: 1.09) solutions in toluene were mixed in the ratio of 40 wt% PS:PMMA, i.e., PS is 40 wt% of PMMA. These PS/PMMA (upper critical solution temperature, UCST is 450 K as estimated from Flory–Huggins Theory[37,38]) blend films of nominally 100 nm average thickness were cast on cleaned silicon wafer (2 h of ultraviolet–ozone treatment) using a custom-built flow coater.[39] The molecular weight and composition of the polymer blend were chosen based on a previous study on fabrication of phase-separated polymer blend structures via spinodal decomposition.[40] The polymer films were coated with silver using Emitech K575x Turbo sputter coater. The optical constants of a 100 nm thick PS and PMMA film were determined using a spectroscopic ellipsometer (M-2000, J.A. Woollam). Surface morphology of the films was characterized using tapping mode in Dimension Icon Atomic Force Microscope (Bruker, AXS). Optical images were taken with Canon PowerShot SX60 HS digital camera with Raynox DCR-250 Super Macro Snap-On Lens and Bestlight® 48 LED Macro Ring Light. Samples were fixed on a rotatable stage, the tilting angle of the stage was measured by Wixey Digital Angle Gauge (WR300 Type 1) before photos were taken.

2.2. UV–Visible Spectroscopy

Normal specular reflectance of the films was measured using a CRAIC AX10 microspectrometer (CRAIC Technologies Inc. 15× objective). Reflectance measurements were normalized using a white Teflon standard. Diffuse reflectance was measured using an integrating sphere (AvaSphere-50-REFL) with a black gloss trap to exclude specular reflectance. All reflectance measurements were taken as percentages relative to a diffuse white standard (WS-2, Avantes). Angle-resolved diffuse reflectance was measured using a spectrometer equipped with two fibres that rotate independently from one another; one fibre was connected to a light source (AvaLight-XE pulsed xenon light) and the other fibre (detector) to a spectrometer (AvaSpec-2048 spectrometer, Avantes Inc., Broomfield, CO, USA). Reflectance was measured between 300 and 700 nm at varying angles (15°–40°) from normal incidence (in order to elucidate optical activity in the UV–visible region). Specular and diffuse reflectance values of the films reported in the figures include the area under the reflectance curve in the wavelength region 300–700 nm in the spectral plot.

3. Results and Discussion

3.1. Preparation of Surface-Roughened Polymer Films

A schematic of preparation of thermally surface-roughened PMMA film (SRPF) on silicon substrate comprised of spinodal-like phase-separated structures of PMMA and air starting from as-cast PS/PMMA blend film is shown in Figure 1a. The as-cast film (ACF) consisted of kinetically trapped nonequilibrium morphology because of the rapid evaporation of the solvent and random distribution of PS nanophase in the PMMA matrix (Figure 1a; Figure S1, Supporting Information). Notably, at micron resolution, such films were uniform in-plane, although a silicon substrate wetting layer of PMMA can be expected. Upon thermal annealing (thermally annealed film, TAF), the PS and PMMA blend components of the film phase-separated through spinodal decomposition, leading to limited roughening of the blend film surface (Figure 1a). In-plane phase separation is largely responsible for the increased roughness of the film. Immersion of these TAFs in cyclohexane selectively removed the PS phase, leaving behind structures comprised of PMMA, and air in place of the PS phase (Figure 1a). Polar interactions between PMMA

© 2017 WILEY-VCH Verlag GmbH & Co. KGaA, Weinheim

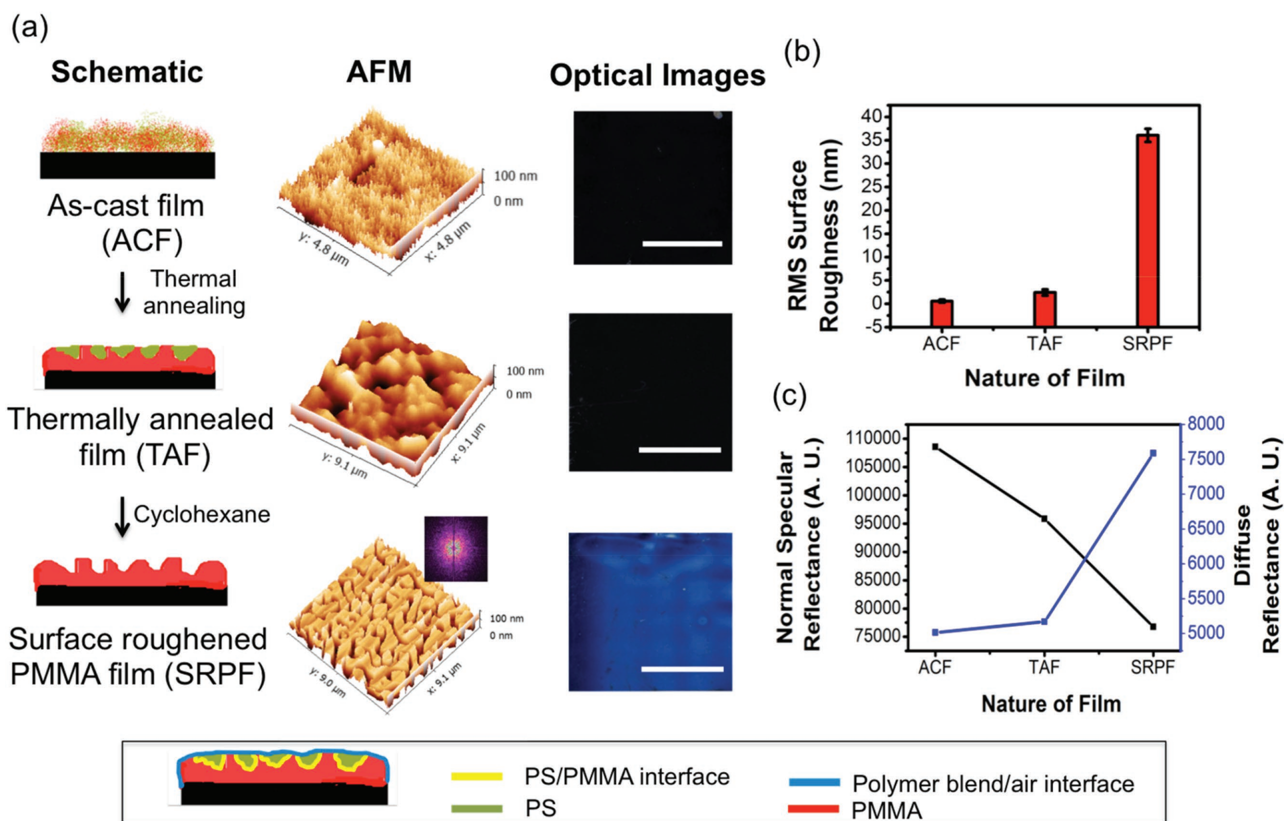

Figure 1. a) Schematic representation of phase separation in PS/PMMA blend film leading to surface-roughened PMMA film (SRPF) comprising of PMMA and air (first column). 3D representation of atomic force microscopic (AFM) images (second column) and optical images (third column) of as-cast (ACF), thermally annealed phase-separated PS/PMMA blend film (TAF), surface-roughened PMMA film (SRPF). Scale bar is 5 mm for optical images. b) RMS surface roughness of as-cast (ACF), thermally annealed (TAF), and surface-roughened PMMA films (SRPF). c) Normal specular and diffuse reflectance in the wavelength region 300–700 nm region of the ACF, TAF, SRPF that were annealed at 150 °C for 2 h.

and hydrophilic silicon substrate presumably enhanced the PMMA wetting layer, which is evident from the nanoscale roughness of the valleys between elevated PMMA domains, while both the polystyrene and polymethylmethacrylate components were present near the polymer–air interface. TAFs consisted of two interfaces: (1) a polymer blend film–air interface and (2) PS–PMMA interface within the blend film. Selective removal of the PS phase from the thermally annealed phase-separated PS/PMMA polymer blend film (TAF) enhanced both surface roughness (Figure 1b), and presumably internal film porosity. Consequently, these highly porous and SRPF are 15 and 60 times rougher than TAF and ACF, respectively (Figure 1b). The refractive-index contrast for the PS–PMMA interface is $n_{PS} - n_{PMMA} = 0.066$, where n is refractive index in TAFs, while $n_{PMMA} - n_{air} = 0.5$ for PMMA–air interface in SRPF at 580 nm (Figure S2, Supporting Information). A fast Fourier transform (FFT) of the atomic force microscope (AFM) images of these SRPF film images indicate an isotropic phase-separated surface morphology (inset in Figure 1a).

3.2. Impact of Surface Roughening on Specular and Diffuse Reflectance

Optical images of the films taken at normal incidence under diffuse incident white light demonstrated that the brightness of SRPF films was higher than that of as-cast and thermally annealed films (Figure 1a). We then measured the normal specular and diffuse reflectance (in the wavelength region 300–700 nm) of films that were annealed at 150 °C for 2 h (Figure 1b). Surface-roughened PMMA films exhibited lower normal specular and higher diffuse reflectance when compared to as-cast and thermally annealed films, because of its rougher surface. ACF and SRPF films exhibited diffuse reflectance of 12.6% and 19%, respectively, relative to the white standard used (Figure S3, Supporting Information).

Since the surface roughness of the films in this case is less than the wavelength of the incident light (300–700 nm), the films were considered relatively smooth or slightly rough. We used the Beckmann and

© 2017 WILEY-VCH Verlag GmbH & Co. KGaA, Weinheim
ADVANCED SCIENCE NEWS
www.advancedsciencenews.com

Spizzichino diffuse reflectance model[41] (B–S DRM) as a reasonable estimate for diffuse reflectance of surface-roughened PMMA films. The intensity of reflected light from a smooth or slightly rough surface according to B–S DRM is given by the following equation

$$\left\langle E_2 E_2^* \right\rangle = \frac{E_{01}^2 A^2 \cos^2\theta_i}{T^2 R_o^2} e^{-g} \left(\rho_o^2 + \frac{\pi \lambda^2 D^2 g}{A} . e^{\frac{-v_{xy}^2 \lambda^2}{4}} \right) \quad (1)$$

where

$$g = \left\{ 2\pi \frac{R_{rms}}{T} (\cos\theta_i + \cos\theta_r) \right\}^2$$

$$\rho_o = -\operatorname{sinc}(v_x X) \operatorname{sinc}(v_y Y)$$

$$D = \left(\frac{1 + \cos\theta_i \cos\theta_r - \sin\theta_i \sin\theta_r \cos\theta_r}{\cos\theta_i (\cos\theta_i + \cos\theta_r)} \right)$$

$$v_{xy} = \sqrt{v_x^2 + v_y^2}$$

The term $\langle E_2 E_2^* \rangle$ corresponds to the intensity of reflected light with local angle of incidence and reflection being θ_i and θ_r, respectively. $R_{rms,}\lambda$, T, v_x, and v_y indicate RMS surface roughness, lateral scale of phase separation (in this case), wavelength of incident light, and velocity of incident light in the X- and Y-directions, respectively. The first term in Equation (1) corresponds to a specular spike indicative of specular reflection, whereas the second term corresponds to a specular lobe indicative of diffuse reflectance. Hence, the increase in diffuse reflectance with increase in surface roughness for normal incidence of light from as-cast and thermally annealed to surface-roughened PMMA films is in agreement with the B–S DRM predictions (Equation (1)).

The effect of casting solvent (toluene, chloroform, and tetrahydrofuran) on phase-separated film morphology and further on diffuse reflectance is shown in Figure S4 (Supporting Information). The morphology of the phase-separated PS/PMMA blend films varied somewhat with casting solvent.[33]

3.3. Impact of Annealing Conditions on Scale of Phase Separation

The lateral scale of phase separation (λ) increased with annealing time from 0.5–3 h (Figure 2a) at a constant annealing temperature (150 °C). The increase in λ of PS/PMMA blend films with annealing time can be attributed to the late-stage coarsening process in polymer blend phase separation. The 2D FFT of the phase-separated structures (inset of Figure 2a) showed that they are isotropic. Along with λ, the root-mean-square surface roughness (R_{rms}) of SRPFs varied with annealing time.

The lateral scale of phase separation (λ) also increased with greater annealing temperatures, which is in congruence with deGenne's theory[42] that the dominant wavelength of phase separation in polymer blends is related to thermal quench depth ($\varepsilon = |T_s - T|$, where T_s is spinodal temperature and T is annealing temperature) as per the following equation (2)

$$\lambda = \varepsilon^{-1/2} \quad (2)$$

As annealing temperature increased, thermal quench depth of polymer blends decreased because of UCST behavior of PS/PMMA blend resulting in longer wavelength fluctuations, i.e, higher λ (Figure 2b). Films annealed at 160 °C for 2 or 3 h had droplet-like morphology and were not studied further. Roughness of surface-roughned PMMA films also varied with lateral scale of phase separation (Figure 2c). The value of "A_s" ($=\lambda \times R_{rms}$) varied with annealing time and temperature (Figure 2d). Therefore, annealing temperature and time can precisely control domain spacing and surface roughness. Governing equations for the phase separation in PS/PMMA blend films studied are given in the Supporting Information.

3.4. Impact of the Scale of Phase Separation on Specular and Diffuse Reflectance

Normal specular reflectance of SRPFs decreased and diffuse reflectance increased with greater surface area, $A_s = \lambda \times R_{rms,}$ wherein λ values ranged from 150–1000 nm and the corresponding R_{rms} values ranged from 1–40 nm (Figure 2e). Since it was difficult to decouple the effect of lateral scale of phase separation (λ) and RMS surface roughness (R_{rms}), the value of "A_s" is taken as an approximate quantitative measure of the "rough surface area" from which diffuse reflectance took place. Diffuse reflectance of SRPF varied from 13% to 20% with change in surface area from 4800 to 25 800 nm^2 (Figure S6, Supporting Information). Therefore, by precisely controlling the lateral scale of phase separation and surface roughness of polymer films, we can control both specular and diffuse reflection.

The term $H = e^{-g}\lambda^2 g e^{-\lambda^2}$ in Beckmann–Spizzichino diffuse reflectance model (Equation (1)) incorporates both the lateral scale of phase separation and surface roughness (in this study) and determines the diffuse reflectance from slightly rough surfaces. Experimental (measured) diffuse reflectance increased with greater surface area A_s for SRPF, and followed a similar trend as theoretical diffuse reflectance ($H \times 10^4$) in this study, thus agreeing with the B–S DRM (Figure 2e). Phase-separated surface-roughened films with an adhesion layer, as provided by the wetting PMMA layer in this case, may be applied as optical adhesive diffusers[43] that can be used in LCDs or LEDs.

© 2017 WILEY-VCH Verlag GmbH & Co. KGaA, Weinheim

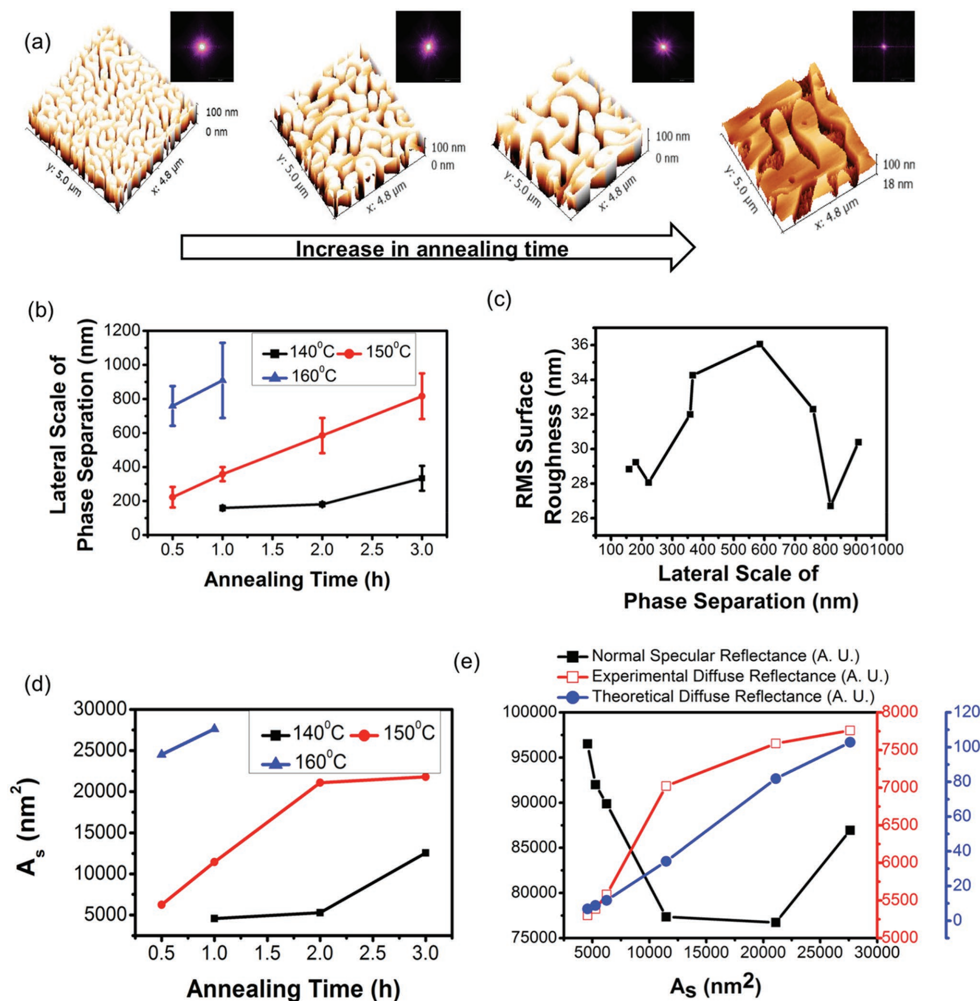

Figure 2. a) AFM height images of surface-roughened PMMA films (SRPF) that were annealed at 150 °C for different annealing times. Inset shows the fast Fourier transform (FFT) of the corresponding AFM images. b) Impact of annealing conditions (time and temperature) on lateral scale of phase separation (λ) in SRPF. c) Variation of RMS surface roughness (R_{rms}) with lateral scale of phase separation (λ) in SRPF. d) Impact of annealing conditions (time and temperature) on rough area "A_s" ($=\lambda \times R_{rms}$). e) Normal specular, experimental, and theoretical diffuse reflectance ($H = e^{-g}\lambda^2 g e^{-\lambda 2}$, based on Beckmann–Spizzichino diffuse reflectance model for slightly rough surfaces) of SRPF with varying rough area "A_s".

3.5. Impact of Silver Coating on Diffuse Reflectance

Diffuse reflectance of visible light was further enhanced by coating surface-roughened PMMA films with a thin metal overlayer (silver in this study), as high reflectance is desirable for practical applications and reflectance from polymer–air, polymer–polymer interfaces is limited, as refractive indices of most of the polymers range from 1.44 to 1.58. However, most of the metals have higher refractive indices than polymers. SRPFs (annealing temperature: 150 °C, annealing time: 2 h) were deposited with a 4.6 ± 2.2 nm thick silver layer, denoted by surface-roughened silver film (SRSF). Prior to AFM and diffuse reflectance experiments after silver deposition, silver would have converted to silver oxide due to oxidation of silver; nominally silver here refers to silver oxide as well. Here, we want to demonstrate the idea that materials with higher refractive index (RI) exhibit higher diffuse reflectance, e.g., silver or silver oxide here. The silver coating did not affect the surface morphology of the film (Figure 3a,b) but reduced the surface roughness of the SRSF compared to that of SRPF due to a planarizing effect (Figure 3c). The silver coating enhanced the intensity of the (diffuse) light by 2.16 times as compared to uncoated, leached blend films (Figure 3d) in the wavelength region 300–700 nm. This is because refractive index contrast for silver–air interface is greater than the PMMA–air interface in the wavelength region of 300–700 nm (local surfaces with normal incidence of light) and is responsible for the increase in intensity of reflected light. For example, RI contrast between PMMA–PS (in TAF), PMMA–air (in SRPF) interface is $n_{PS} - n_{PMMA} = 0.066$, $n_{PMMA} - n_{air} = 0.5$ (at 580 nm), respectively, and is lower than RI contrast

© 2017 WILEY-VCH Verlag GmbH & Co. KGaA, Weinheim
ADVANCED SCIENCE NEWS
www.advancedsciencenews.com

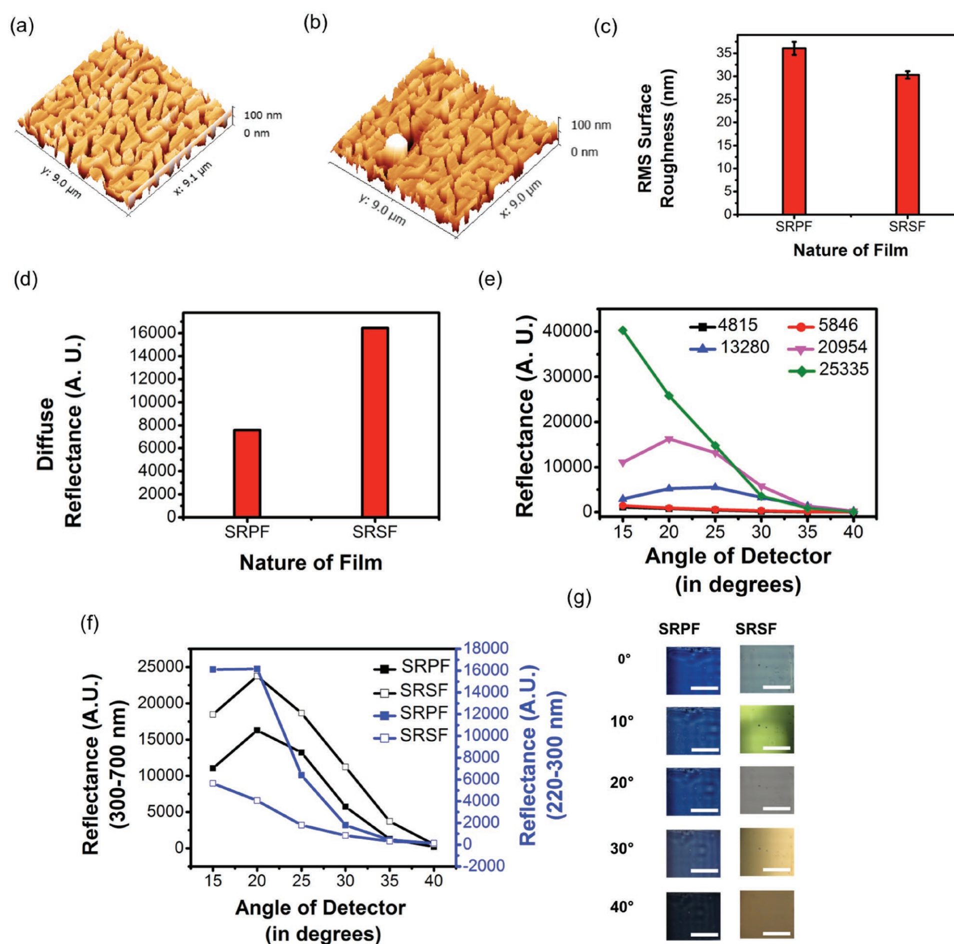

Figure 3. AFM height images of (a) surface-roughened PMMA (SRPF) and (b) surface-roughened silver (SRSF) films, respectively, that were annealed at 150 °C for 2 h. RMS surface roughness and diffuse reflectance of (c) SRPF and (d) SRSF. Angle-resolved diffuse reflectance of (e) surface-roughened polymer films (SRPF) at various rough areas (A_s). (f) Surface-roughened PMMA (SRPF) and surface-roughened silver (SRSF) films that were annealed at 150 °C for 2 h in the wavelength region 220–300 nm and 300–700 nm. (g) Optical images of SRPF and SRSF corresponding to the graph in panel (f) that were annealed at 150 °C for 2 h. Scale bar is 5 mm for optical images.

between silver–air interface ($n_{silver} - n_{air} = 2.97$ at 580 nm) in SRSF.

3.6. Angle-Resolved Diffuse Reflectance

Angle-resolved diffuse reflectance of surface-roughened PMMA films varied with surface area A_s for normal incidence of light (azimuthal angle is constant in this case) (Figure 3e). The spectral dependency of SRPF is shown in Figure S7 (Supporting Information). The intensity of diffusively reflected light depended on angle of observation (studied up to 40° from normal incident light direction) and increased with increase in "A_s"(Figure 3e), thus placing it under the category of non-Lambertian surfaces (in a Lambertian surface, light is reflected uniformly in all the directions and vice versa). Nonuniform diffuse reflectance is observed in those cases where reflectance primarily depends on the surface structure. The Beckmann and Spizzichino diffuse reflectance model (Equation (1)) also suggests that for normal incidence of light, intensity of reflected light depends on angle of observation. Therefore, we understand that light diffusivity can be imparted to the films and can be controlled by incorporating varying degrees of surface roughness and lateral scales of phase separation, parameters that can control the intensity of the diffusively reflected light. Furthermore, silver coating enhanced reflectance of SRPF in the 300–700 nm wavelength region as compared to uncoated surface-roughened polymer films (Figure 3f). Notably, in the wavelength region of 220–300 nm, we see a lower reflectance from silver-coated film compared to uncoated film that is related to the extinction coefficient of silver (220–300 nm wavelength region) (Figure S2, Supporting Information). It is interesting to note that at 40° from surface normal, the intensity of diffusively reflected light from silver-coated film decreased with increase in angle of detector (Figure 3g).

© 2017 WILEY-VCH Verlag GmbH & Co. KGaA, Weinheim

4. Conclusions

In summary, these are the first reports of the optical activity of spinodal phase-separated nanoroughened polymer blend thin films. The blend is comprised of PS/PMMA derived PMMA/air films analogous to porous phase-separated structures in nature. Our studies demonstrated that nanoroughened PMMA films exhibited enhanced diffuse reflectance relative to as-cast and thermally annealed phase-separated films that are relatively smooth. The diffuse reflectance increased with greater surface-roughened area as controlled by phase separation parameters. Coating the surface-roughened PMMA film with a thin conformal silver coating further enhanced (300–700 nm) and attenuated (220–300 nm) the intensity of diffuse reflection. Angle-resolved diffuse reflectance showed that the light is reflected in a nonuniform fashion at various angles from the incident normal, classifying it as a non-Lambertian surface. These films may be useful as diffuse reflectors in, for example, solar panels.

Supporting Information

Supporting Information is available from the Wiley Online Library or from the author.

Acknowledgements: The authors would like to acknowledge the funding sources from National Science Foundation Division of Materials Research (NSF-DMR, Grant no. 1411046), Air Force Office of Scientific Research (AFOSR, Grant nos. FA9550-16-1-0331 and FA9550-13-1-0222), Human Frontiers Science Program (HFSP RGY-0083) and Fonds Wetenschappelijk Onderzoek (FWO G007117N). The authors would like to acknowledge Bor-kai Hsiung for helping with the optical images of the films, Sonal Bhadauriya for helping with the Ellipsometer measurements. The authors would like to thank Ming Xiao, Liliana D'Alba, Brani Igic, Arvind Modi, Sarang Bhaway, Ren Zhang, Daphne Fecheyr-Lippens, Jennifer Peteya, Namrata Salunke, Nicholas Justyn, Monali Basutkar, Sukhmanjot Kaur for various helpful discussions and their comments on the manuscript. The authors sincerely acknowledge the reviewers for their insightful comments that helped improve the manuscript.

Received: December 23, 2016; Revised: February 14, 2017; Published online: April 6, 2017; DOI: 10.1002/marc.201600803

Keywords: diffuse reflectance; optics; phase separation; polymer blends; surface roughening

[1] S. H. Lee, T. Yoon, J. C. Kim, *Opt. Lett.* **2006**, *31*, 2196.
[2] Y. J. Lee, H. C. Kuo, T. C. Lu, S. C. Wang, *IEEE J. Quantum Electron.* **2006**, *42*, 1196.
[3] J. K. Kim, J. Q. Xi, H. Luo, E. F. Schubert, J. Cho, C. Sone, Y. Park, *Appl. Phys. Lett.* **2006**, *89*, 141123.
[4] H. Kim, S. N. Lee, Y. Park, K. K. Kim, J. S. Kwak, T. Y. Seong, *J. Appl. Phys.* **2008**, *104*, 053111.
[5] K. H. Lee, Y. T. Moon, J. O. Song, J. S. Kwak, *Sci. Rep.* **2015**, *5*, 1.
[6] A. Banerjee, S. Guha, *J. Appl. Phys.* **1991**, *69*, 1030.
[7] J. E. Cotter, *J. Appl. Phys.* **1998**, *84*, 618.
[8] L. M. Farrier, *Masters Thesis*, Air Force Research Laboratory (Wright-Patterson Air Force Base-Ohio) **2006**.
[9] P. Fedders, *Phys. Rev.* **1969**, *181*, 1053.
[10] D. Fuellemann, R. Mauser, R. Specht, M. Stauch, H. Oelkrug, *J. Mol. Struct.* **1986**, *143*, 251.
[11] C. S. West, K. A. O'Donnell, *Phys. Rev. B* **1999**, *59*, 2393.
[12] A. Roos, M. Bergkvist, C. G. Ribbing, *Thin Solid Films* **1988**, *164*, 5.
[13] K. Kamoshida, *J. Vac. Sci. Technol. B* **2000**, *18*, 2565.
[14] S. Il Chang, J. B. Yoon, H. Kim, J. J. Kim, B. K. Lee, D. H. Shin, *Opt. Lett.* **2006**, *31*, 3016.
[15] T. Wei, Q. Kong, J. Wang, J. Li, Y. Zeng, G. Wang, J. Li, Y. Liao, F. Yi, *Opt. Express* **2011**, *19*, 1065.
[16] R. Dylewicz, A. Z. Khokhar, R. Wasielewski, P. Mazur, F. Rahman, *Appl. Phys. B: Lasers Opt.* **2012**, *107*, 393.
[17] J. Y. Cho, S. H. Hong, K. J. Byeon, H. Lee, *Thin Solid Films* **2012**, *521*, 115.
[18] S. Chhajed, W. Lee, J. Cho, E. F. Schubert, J. K. Kim, *Appl. Phys. Lett.* **2011**, *98*, 071102.
[19] J. S. Ahn, T. R. Hendricks, I. Lee, *Adv. Funct. Mater.* **2007**, *17*, 3619.
[20] K. Michielsen, D. G. Stavenga, *J. R. Soc., Interface* **2008**, *5*, 85.
[21] K. Michielsen, H. De Raedt, D. G. Stavenga, *J. R. Soc., Interface* **2010**, *7*, 765.
[22] V. Saranathan, C. O. Osuji, S. G. J. Mochrie, H. Noh, S. Narayanan, A. Sandy, E. R. Dufresne, R. O. Prum, *Proc. Natl. Acad. Sci. USA* **2010**, *107*, 11676.
[23] E. R. Dufresne, H. Noh, V. Saranathan, S. G. J. Mochrie, H. Cao, R. O. Prum, *Soft Matter* **2009**, *5*, 1792.
[24] C. Lee, J. J. Kim, *Small* **2013**, *9*, 3858.
[25] R. Liu, Z. Ye, J. M. Park, M. Cai, Y. Chen, K. M. Ho, R. Shinar, J. Shinar, *Opt. Express* **2011**, *19*, A1272.
[26] A. M. Higgins, R. A. L. Jones, *Nature* **2000**, *404*, 476.
[27] P. Adelhelm, Y. S. Hu, L. Chuenchom, M. Antonietti, B. M. Smarsly, J. Maier, *Adv. Mater.* **2007**, *19*, 4012.
[28] S. Walheim, E. Schaffer, J. Mlynek, U. Steiner, *Science* **1999**, *283*, 520.
[29] N. Wang, X. Chen, Y. Yang, J. Dong, C. Wang, G. Yang, *Sci. Rep.* **2013**, *3*, 1.
[30] D. U. Ahn, Z. Wang, I. P. Campbell, M. P. Stoykovich, Y. Ding, *Polymer* **2012**, *53*, 4187.
[31] S. Walheim, M. Böltau, J. Mlynek, G. Krausch, U. Steiner, *Macromolecules* **1997**, *30*, 4995.
[32] D. A. Winesett, H. Ade, J. Sokolov, M. Rafailovich, S. Zhu, *Polym. Int.* **2000**, *49*, 458.
[33] L. Cui, Y. Ding, X. Li, Z. Wang, Y. Han, *Thin Solid Films* **2006**, *515*, 2038.
[34] A. Karim, T. M. Slawecki, S. K. Kumar, J. F. Douglas, S. K. Satija, C. C. Han, T. P. Russell, Y. Liu, R. Overney, O. Sokolov, M. H. Rafailovich, *Macromolecules* **1998**, *31*, 857.
[35] K. Dalnoki-Veress, J. A. Forrest, J. R. Stevens, J. R. Dutcher, *Physica A* **1997**, *239*, 87.
[36] X. Li, Y. Han, A. Lijia, *Appl. Surf. Sci.* **2004**, *230*, 115.

© 2017 WILEY-VCH Verlag GmbH & Co. KGaA, Weinheim

[37] F. S. Bates, *Science* **1991**, *25*, 898.
[38] T. P. Russell, R. P. Hjelm Jr., P. A. Seeger, *Macromolecules* **1990**, *23*, 890.
[39] C. M. Stafford, K. E. Roskov, T. H. Epps III, M. J. Fasolka, *Rev. Sci. Instrum.* **2006**, *77*, 023908–1.
[40] R. Zhang, B. Lee, M. R. Bockstaller, S. K. Kumar, C. M. Stafford, J. F. Douglas, D. Raghavan, A. Karim, *Macromolecules* **2016**, *49*, 3965.
[41] P. Beckmann, A. Spizzichino, *The Scattering of Electromagnetic Waves from Rough Surfaces*, Artech House, Inc., Norwood, MA **1987**.
[42] P. G. de Gennes, *J. Chem. Phys.* **1980**, *72*, 4756.
[43] R. J. Goetz, A. J. Ouderkirk *3M Innovative Properties Company*, *US 6288172 B1*, **2001**.
[44] K. Tanaka, A. Takahara, T. Kajiyama, *Macromolecules* **1998**, *31*, 863.

© 2017 WILEY-VCH Verlag GmbH & Co. KGaA, Weinheim